

A Novel Nitidine Chloride Nanoparticle Inhibits the Stemness of CD133⁺EPCAM⁺ Huh7 Hepatocellular Carcinoma Cells

Danni Li¹, Qiyang Zhang¹, Yuzhu Zhou¹, Hua Zhu^{2*}, Tong Li^{2*}

¹School of Chemistry and Chemical Engineering, Guangxi University for Nationalities, Nanning, Guangxi Province, China

²College of Pharmacy, Guangxi University for Chinese medicine, Guangxi Province, China

ABSTRACT

Nitidine chloride is a natural product. We synthesized novel nanoparticles of Nitidine chloride (TPGS-FA/NC), which evaluated anti-hepatocellular carcinoma potential capability *in vitro* and *in vivo*. Cell viability was assessed by MTT and colony assays; TPGS-FA/NC was examined by Confocal Microscopy through targeting Huh7 Hepatocellular Carcinoma Cells. A sphere culture technique was used to enrich Cancer Stem Cells (CSC) in Huh7 cells. The *in vivo* antitumor efficacy of TPGS-FA/NC was evaluated in Huh7 cell xenograft model, which were administered by TPGS-FA/NC for 2 weeks. TPGS-FA/NC (10, 20, 40 µg/mL) dose-dependently inhibited the proliferation of HCC cells. Interestingly, TPGS-FA/NC (10, 20, 40 µg/mL) drastically reduced the EpCAM⁺/CD133⁺ cell numbers, which suppressed the sphere formation and inhibited the expression of stem cell marker in the Huh7 spheroids. Additionally, TPGS-FA/NC time-dependently suppressed the AQP3/CD133/STAT3/JAK signalling pathways in Huh7 cells. In Huh7 cells xenograft bearing nude mice, TPGS-FA/NC administration significantly

inhibited the tumour growth and markedly reduced the number of cancer stem-like cells in the tumours. TPGS-FA/NC treatment also reduced the expression of stem cell markers. The novel nitidine chloride nanoparticles markedly inhibited the HCC tumour growth through multiple mechanisms, and it may be a potential candidate drug for the therapy of hepatocellular carcinoma.

Key Words: Nitidine chloride, Nano-micelles, Cancer stem cells, Xenograft nude mice model, AQP3/STAT3/JAK pathway

Correspondence:

Hua Zhu, College of Pharmacy, Guangxi University for Chinese medicine, No.13, Wu He street, Qingxiu District, Nanning, 530200, Guangxi Province, China, E-mail: che_2020@163.com

Tong Li, College of Pharmacy, Guangxi University for Chinese medicine, No.13, Wu He street, Qingxiu District, Nanning, 530200, Guangxi Province, China, E-mail: litong202110@163.com

INTRODUCTION

The Cancer Stem Cells (CSC) is identified as stem cell properties, which revealed the existence of CSC in HCC [1,2]. The research suggested that CD133⁺EpCAM⁺ phenotype precisely represented the characteristics of CSC in Huh7 cells [3–7]. Currently some chemotherapeutic drugs primarily inhibit the growth of differentiated tumour cells with no impact on CSC [8,9].

Recent studies have shown that expression of AQP3 resulted in the progression and metastasis of several malignant tumours [10–13]. Many researches reveal that AQP3 is related to the maintenance of stemness in Cancer Stem Cells (CSCs) [14–16]. The research shows that a novel mechanism of AQP3/STAT3/CD133 pathway in HCC was demonstrated [16]. A member of the Nek family of serine/threonine kinases (NIMA-related kinase2) is markedly associated with the essential mitotic regulator, which is highly expressed at the centrosome [17]. Furthermore, experimental evidence shows that Nek2 could predict treatment resistance in hepatocellular carcinoma [18]. The previous study showed that we synthesized nitidine chloride nanoparticles (TPGS-FA/NC) successfully [19]. We demonstrate the mechanisms of TPGS-FA/NC inhibit the growth of EpCAM⁺/CD133⁺ Huh7 cells *in vitro* and *in vivo* via AQP3/STAT3/CD133 signal pathway further.

METHODOLOGY

Chemicals and antibodies

TPGS-FA/NC was synthesized in our laboratory and dissolved in DMSO. Recombinant Human basic fibroblast growth factor was purchased from Beijing Solarbio Science and Technology Co., Ltd. (Solarbio, Beijing, China) and recombinant human1 Epidermal Growth Factor (EGF) was acquired from Shanghai Yuanye Biotechnology Corporation (Yuanye, Shanghai, China). DMEM/F-12 Life were purchased from Procell Science and Technology Co., Ltd. (Procell, Wuhan, China). B27 (X50) were purchased from thermofish Scientific (Thermofish, Waltham, USA) and Insulin-Transferrin-Selenium (ITS × 100), L-glutamine (X100) was purchased from Procell Science and Technology Co., Ltd. (Procell, Wuhan, China). The anti-CD133 (AC133)-phycoerythrin (PE) and anti-CD326 (EpCAM)-Allophycocyanin (APC) antibodies and isotype-matched mouse anti-IgG1-PE and anti-IgG1-APC were purchased from Miltenyi Biotec (North Rhine-Westphalia, Germany). Antibodies

against phosphoSTAT3 (Tyr705), STAT3, JAK1, JAK2, AQP3 and Glyceraldehyde Phosphate Dehydrogenase (GAPDH) were purchased from the Beijing Solarbio Science and Technology Co., Ltd. (Solarbio, Beijing, China). Glyceraldehyde phosphate dehydrogenase (GAPDH) was purchased from the Beijing Solarbio Science and Technology Co., Ltd. (Solarbio, Beijing, China). The DMEM/F-12, anti-rabbit and anti-mouse secondary antibodies were purchased from Procell Science and Technology Co., Ltd. (Procell, Wuhan, China). DAPI was obtained from Shanghai Beyotime Biotechnology Co. Ltd. (Beyotime, Shanghai, China). The iFluor™ 647 phalloidin iFluor™ were purchased from Yeasen Biotechnology Co., Ltd (Yeasten, Shanghai, USA).

Cell culture

The Huh7 human hepatoma cell lines were provided by the Shanghai Cell Bank (Shanghai Institute for Biological Science, Chinese Academy of Science, Shanghai, China). Huh7 cells were cultured in DMEM supplemented with 10% FBS, 100 U/mL penicillin, and 50 mg/mL streptomycin at 37°C in a humidified 5% CO₂ incubator.

Tumour sphere formation assay and flow cytometric analysis sphere cultures were performed as previously described with minor modifications [9]. Briefly, primary sphere cells were obtained by culturing HCC cells in sphere-forming conditioned DMEM/F12, supplemented with FGF (20 ng/mL), EGF (20 ng/mL), B27 (1X), and L-glutamine (1X) in 6-well ultra-low attachment plates. The primary sphere cells (1 × 10³ cells/well) were incubated with or without TPGS-FA/NC for 7 d. The second and third passages of the cells were grown for 7 d in the absence of TPGS-FA/NC. To examine TPGS-FA/NC effects on the subpopulation of cells that expressed EpCAM and CD133, cells were incubated with anti-AC133-PE and anti-EpCAM-APC antibodies and analysed by flow cytometry. Isotype-matched mouse anti-IgG1-PE and anti-IgG1-APC were used as controls.

This is an open access article distributed under the terms of the Creative Commons Attribution Noncommercial Share Alike 3.0 License, which allows others to remix, tweak, and build upon the work non commercially, as long as the author is credited and the new creations are licensed under the identical terms.

For reprints contact: pharmacy@jbcplpharm.org

Cite this article as: Li D, Zhang Q, Zhou Y, et al. A Novel Nitidine Chloride Nanoparticle Inhibits the Stemness of CD133⁺EPCAM⁺ Huh7 Hepatocellular Carcinoma Cells. J Basic Clin Pharma 2021;12:113-119.

Confocal microscopy imaging

Huh7 cells were seeded on glass cover-slips and cultured at 37°C overnight. Rhodamine B iso thiocyanate 540 labelled TPGS-FA/NC were incubated with cells at a final concentration of 100 nm for 4 h at 37°C. After washing twice with PBS buffer, cells were fixed with 4% formaldehyde and washed again, followed by treatment with 0.1% Triton X-100 in PBS buffer for 5 min and subsequent cytoskeleton staining with iFluor™ 647 phalloidin iFluor™ for 30 min at room temperature containing DAPI for cell nucleus staining and assayed on Leica SP8 confocal microscope (Leica Corp.).

Western blot

Western blot methods were performed as previously described [18].

Immuno histochemistry (IHC)

AQP3/CD133/EPCAM/NEK2 expression was analysed in paraffin-embedded specimens obtained from nude mice tumour tissue. Tissue sections were incubated with anti-AQP3 (1:100, Solarbio), anti-CD133 (1:100, Solarbio), anti-EPCAM (1:100, Solarbio), and anti-NEK2 (1:100, Solarbio) overnight at 4°C. Then, the sections were incubated with biotinylated goat anti-rabbit IgG as a secondary antibody (Zhongshan Kit, China) for 30 min at 37°C. The specimens were assessed three times.

In vivo bio distribution study

Rhodamine B iso thiocyanate labelled TPGS-FA/NC (2 mg.kg⁻¹, NC per body weight) were systemically administered *via* the tail vein into Huh7 tumour bearing mice. PBS-injected mice were used as fluorescence negative controls. The whole-body imaging of mice was conducted at 8 h using an IVIS system (XMRS) with excitation at 535 nm and emission at 694 nm. The mice were sacrificed at 8 h post-injection by the inhalation of CO₂ followed by cervical dislocation, and major organs were collected and subjected to fluorescence imaging for the assessment of bio distribution profiles. The fluorescence imaging data of average radiant efficiency ((ps⁻¹cm⁻²sr⁻¹)(μWcm⁻²)⁻¹) were quantitative by IVIS system (XMRS) program.

Magnetic-Activated Cell Sorting (MACS) analyses were used to isolate EpCAM and CD133 Huh7 cells determine cell number, Centrifuge cell suspension at 300×g for 10 minutes. Aspirate supernatant completely. Re-suspend cell pellet in 300 μL of buffer per 5 × 10⁷ total cells. Add 100 μL of FcR blocking reagent per 5 × 10⁷ total cells and mix well. Add 100 μL of EpCAM microbeads per 5 × 10⁷ total cells. Mix well and incubate for 30 minutes in the refrigerator (2°C–8°C). Wash cells by adding 5–10 mL of buffer per 5 × 10⁷ cells and centrifuge at 300 × g for 10 minutes. Aspirate supernatant completely and suspend up to 106 cells in 500 μL buffer. Proceed to magnetic separation, EpCAM Huh7 cells were collected. Followed above methods, EpCAM Huh7 cells were sorted after CD133 microbeads incubation. EpCAM⁺ and CD133⁺ Huh7 cells were collected by magnetic separation.

In vivo tumour inhibition by TPGS-FA/NC nanoparticles

Freshly sorted CD133⁺ EpCAM⁺ cells were collected in sterile DMEM without FBS. 200 μL cell suspension, mixed with matrigel (BD Biosciences, CA) (1:1), was subcutaneously injected into each BALB/c nude mice, which were randomly divided into four groups (n=5 biologically independent animals). Samples were administrated by IV

injection in a total of 5 doses (4 mg kg⁻¹, NC per body weight) every other day. Tumour volume, calculated as (length × width²)/2, and mouse weight were monitored every other day. Data were statistically analysed by two-tailed unpaired t-test and presented as mean ± SD; *p<0.05; **p<0.01; ***p<0.001.

Statistics

Statistical differences were evaluated using two-tailed unpaired t-test with Graph Pad software, and statistically significant differences are denoted as *p<0.05, **p<0.01, and ***p<0.001. No adjustments were made for multiple comparisons.

RESULTS

Cell proliferation

Huh7 cells (2 × 10³ cells/well) were seeded into 96-well plates and treated with TPGS-FA/NC (0–120 μg/mL) for 24, 48, and 72 h (Figure 1). Cell proliferation was assessed using MTT in a concentration and time-dependent manner.

TPGS-FA/NC inhibits hepatic cancer stem-like cells

To investigate whether TPGS-FA/NC suppressed HCC CSCs, we enriched the hepatic CSC populations in the Li-7 and Huh7 cell lines using the sphere culture technique. The flow cytometric analysis demonstrated that the EpCAM⁺/CD133⁺ cells accounted for 82.0% of the Huh7 sphere cells, respectively. TPGS-FA/NC (10, 20 and 40 μg/mL) potentially reduced the fraction of EpCAM⁺/CD133⁺ cells (Figure 2a).

TPGS-FA/NC inhibits hepatoma cell proliferation and colony formation

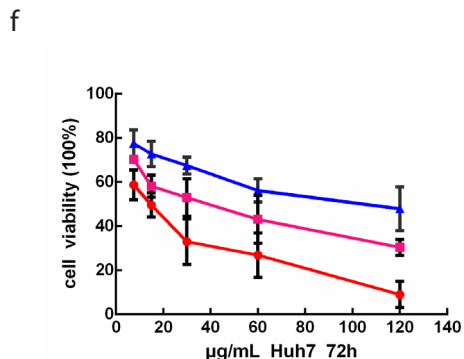
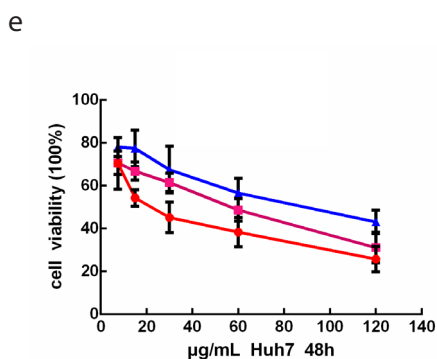
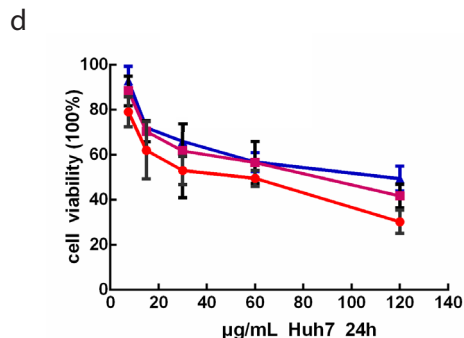
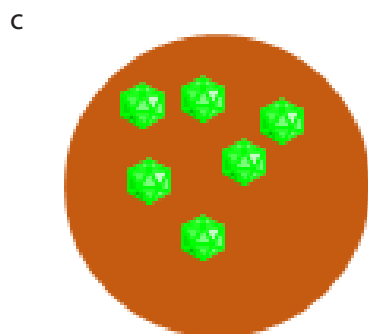
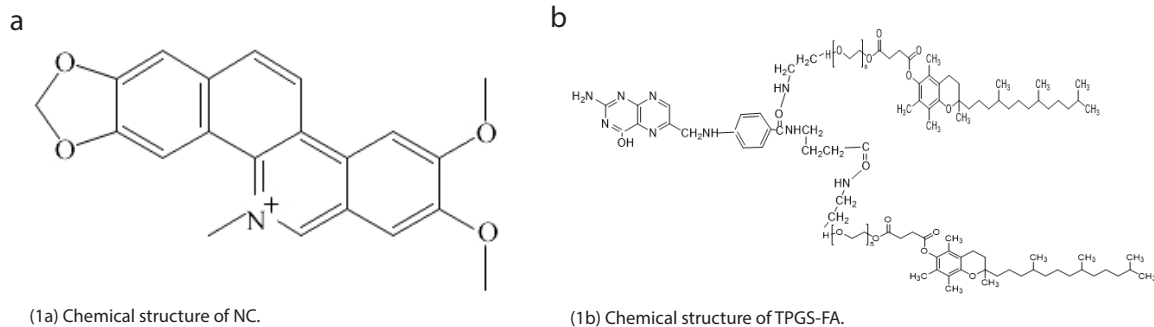
HCC cells (1 × 10³ cells/well) were treated with or without TPGS-FA/NC in 6-well Ultra-Low Attachment Microplates and allowed to grow for 17 to 21 days. The TPGS-FA/NC treatment inhibited Huh7 cell proliferation and also markedly reduced the number of colonies in the clonogenic assays (Figure 2b).

TPGS-FA/NC impair NEK2/CD133/EpCAM signalling of HCC

The protein levels of NEK2, CD133 and EpCAM were determined in cells and nude mice treated with and without TPGS-FA/NC. TPGS-FA/NC successfully reduced protein expression levels of NEK2, CD133 and EpCAM in HCC. *In vivo* experiment, we tested the CD133 and AQP3 expression levels in sections of nude mice subcutaneous tumours by IHC, results showed TPGS-FA/NC downregulated NEK2, CD133 and EpCAM protein levels (Figure 3).

TPGS-FA/NC suppresses the AQP/CD133/STAT pathways

Several studies have shown that the JAK/STAT3 signalling pathway contributed to the induction and maintenance of CSCs *via* the transcriptional regulation of CD133. TPGS-FA/NC reduced the protein expression levels of JAK1, JAK2, pY705-STAT3, STAT3. Furthermore, TPGS-FA/NC reduced the AQP3 protein expression, which suppressed the expression of activated STAT3 (pY705-STAT3) (Figure 4). Then, *in vivo* experiment, we tested the CD133 and AQP3 expression levels in sections of nude mice subcutaneous tumours by IHC, results showed TPGS-FA/NC downregulated AQP3 and CD133 protein levels.



(1e) TPGS-FA/NC inhibited Li-7Huh7 cell proliferation as determined by the MTT assay in 48 hours, n=3.

(1f) TPGS-FA/NC inhibited Li-7Huh7 cell proliferation as determined by the MTT assay in 72 hours, n=3.

Figure 1: The effects of TPGS-FA/NC on Huh7 cell proliferation and colony formation. **Note:** (●) TPGS-FA/NC; (■) NC; (▲) 5-u
Note: *p<0.05 vs. control.

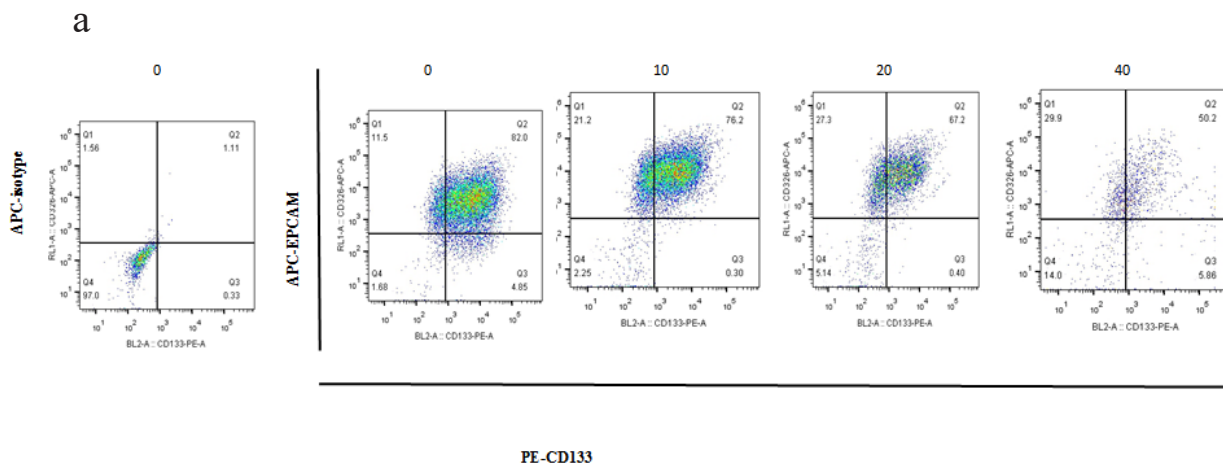


Figure 2a: TPGS-FA/NC reduced the population of EpCAM⁺/CD133⁺ cells in the spheres treated with TPGS-FA/NC for 48 h.

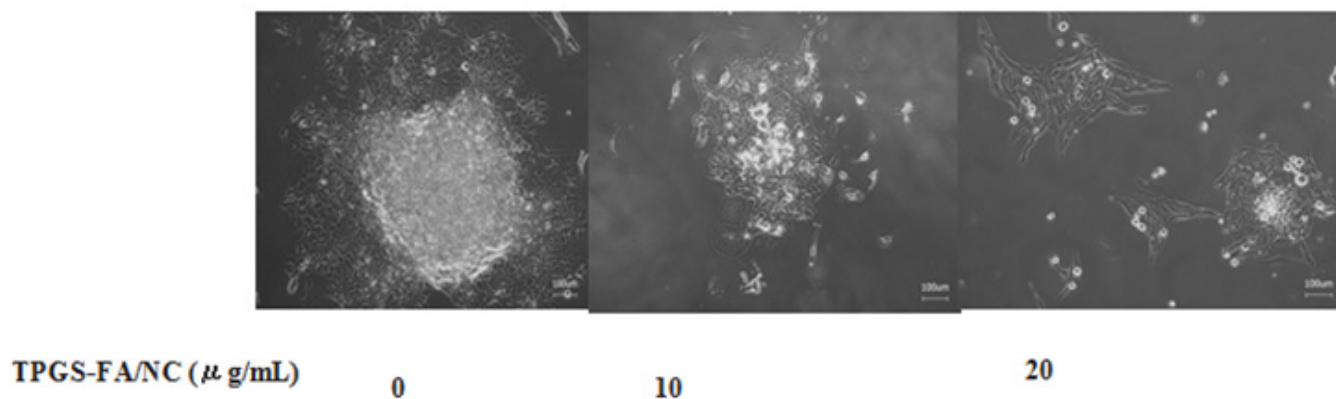


Figure 2b: TPGS-FA/NC reduced the sizes Huh7 primary spheres (magnification X400).

a

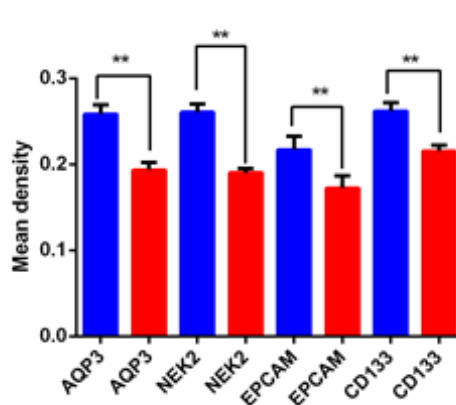


Figure 3a: The effects of TPGS-FA/NC on hepatic cancer stem-like cells. **Note:** (■) TPGS-FA/NC; (■) PBS

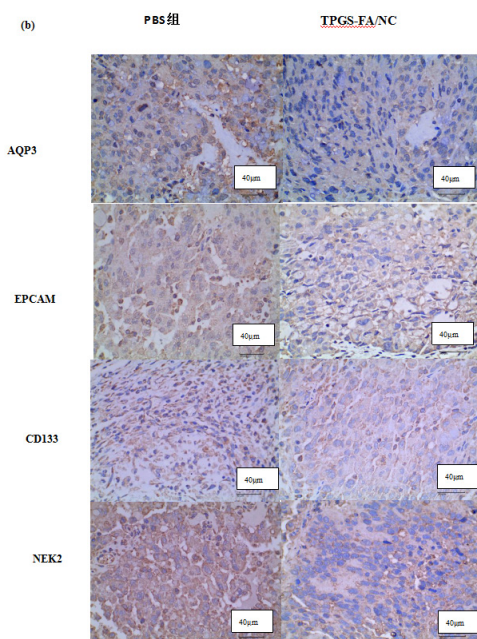


Figure 3b: The protein expressions of AQP3, NEK2, EPCAM, and CD133 (X200) were mainly located in cyto membrane according to IHC in 30 HCC mice bearing Huh7 xenograft specimens.

Note: **p<0.01

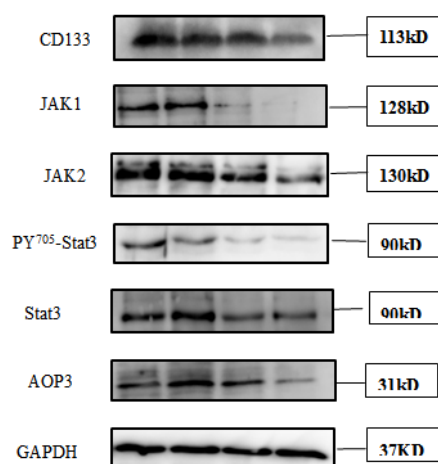


Figure 4: TPGS-FA/NC nanoparticles regulates CD133 and PY705-STAT3 protein by AQP3 proteins expression of DMSO, TPGS-FA/NC:10 µg/mL, 20 µg/mL, 40 µg/mL.

Significant inhibition of tumour by TPGS-FA/NC nanoparticles

To evaluate nanoparticles targeting tumour capability, the Rhodamine B isothiocyanate 540 fluorophore was attached to TPGS-FA. Confocal microscope imaging showed that TPGS-FA/NC nanoparticles entered the Huh7 cells *in vitro*, compared with the control groups (Figure 5).

Tumour quantitative bio distribution and targeting of the TPGS-FA/NC were assessed, which were injected through the tail vein *in vivo*. Those images of mice 8 h post-injection showed that the TPGS-FA/NC nanoparticles markedly accumulated in tumour, with low or no accumulation in brain, heart, spleen. (Figure 6a). Quantitative analysis of the organ images showed strongly tumour accumulation. (Figure 6b). After injecting with TPGS-FA/NC at a dose of 4 mg/kg⁻¹ (NC per mouse weight) every 2 days for a total of five dosages, the results revealed an inhibitory capability *in vivo* as administration by tumour volumes, whereas control group (Figure 6c). The specific tumour inhibition was further confirmed from the tumours harvested after 2-week post injections. Those nanoparticles were biocompatible, which showed no obvious organ toxicity over two-week post injections (Figure 6d).

DISCUSSION

In this study, we enriched populations of hepatic cancer stem-like cells by using a sphere culture technique. Huh7 cells easily formed spheroid

colonies after being cultured with serum-free media, which exhibited self-renewal capacities and expressed CSC membrane biomarkers (EpCAM and CD133). We revealed that TPGS-FA/NC markedly decreased the positive EpCAM/CD133 cell population as identified by FACS analysis, which appeared to be associated with a suppressed self-renewal capability of these cancer stem-like cells. TPGS-FA/NC markedly reduced the numbers and sizes of the spheres. Importantly, the TPGS-FA/NC *in vitro* activity on hepatic cancer stem-like cells was substantiated by our *in vivo* experiments at a dose of 4 mgkg⁻¹ treatment for 14 d significantly inhibited Huh7 xenograft tumour growth. This might provide a novel target or method for the treatment of HCC in the future. According to these studies, we showed that TPGS-FA/NC suppressed the AQP3/STAT3/CD133 pathway in HCC cells, which was evidenced by reduced phosphorylation of STAT3 (pY705-STAT3) as well as inhibiting the expression of AQP3 and downregulated the expression of CD133. The results showed, the downregulation of the AQP3/STAT3/CD133 pathway might have contributed to the inhibitory effect of TPGS-FA/NC on hepatic CSCs. We also found that TPGS-FA/NC reduced the expression of NEK2, which suppressed the expression of protein of EpCAM, and CD133 in Huh7 cells. This results reveals that the TPGS-FA/NC inhibit cell growth in Huh7 cells, which are correlated with the carcinogenic molecular mechanism of AQP3/STAT3/CD133 signalling pathway. In conclusion, we demonstrate that TPGS-FA/NC are an effective inhibitor of HCC tumour growth with low toxicity (Figure 7).

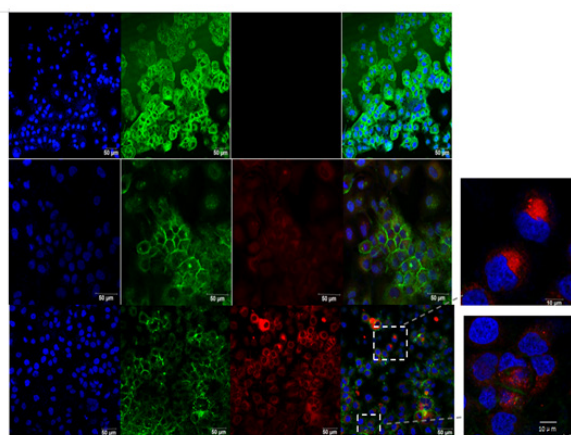


Figure 5: *In vitro* Huh 7 cells binding of TPGS-FA/NC nanoparticles, shown by confocal microscopy.

Note: blue: nucleus; green: cytoskeleton; red: TPGS-FA/NC nanoparticles scale bar: 50 µm for original images and 10 µm for magnified image.



Figure 6a: Representative organ images showing specific tumour targeting of rhodamine B iso thiocyanate labelled TPGS-FA/NC nanoparticles 8 h post-injection into mice bearing Huh7 xenograft ($\text{p s}^{-1} \text{cm}^{-2} \text{sr}^{-1}$) (μWcm^{-2})⁻¹ V.

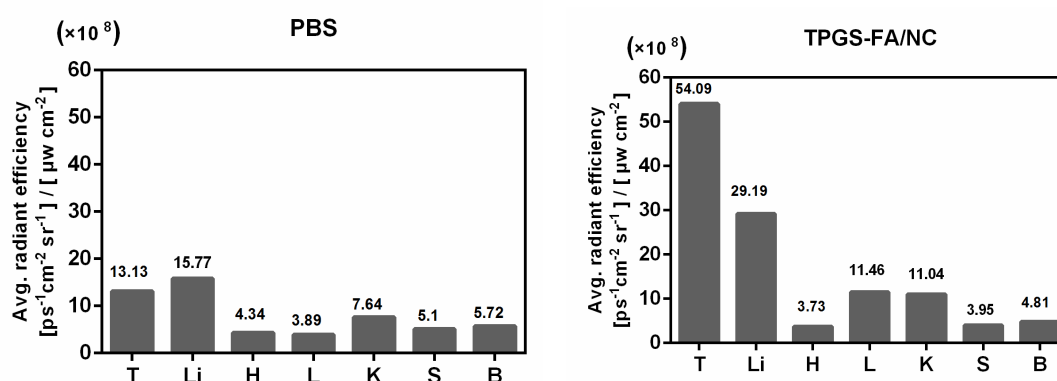


Figure 6b: Quantitative analysis of bio distribution in tumours and normal organs, quantified from the organ images.

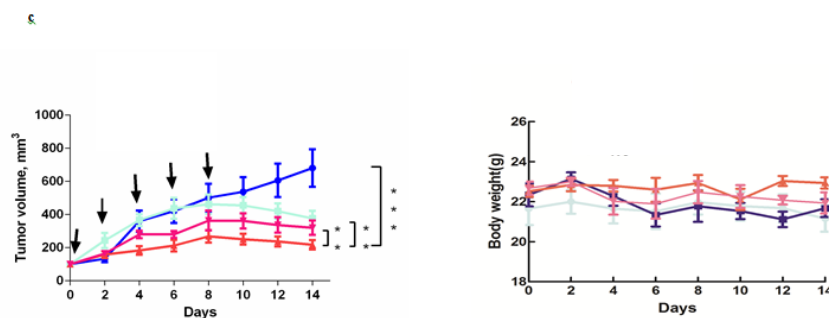


Figure 6c: Intravenous treatment of nude mice bearing ortho topic Huh7 xenografts with TPGS-FA/NC nanoparticles (red) and control groups (turquoise: NC, fuchsia: 5-Fu, blue: PBS) every other day for a total of five injections (4 mg kg^{-1} , NC per body weight, indicated by arrows). ($n=5$ biologically independent animals, statistics was calculated by two-tailed unpaired t-test presented as mean \pm SD, * $p<0.05$, ** $p<0.01$, *** $p<0.001$, $p=4.3 \times 10^{-3}$, 3.4×10^{-3} and 5.0×10^{-4} comparing TPGS-FA/NC to NC, 5-Fu and PBS, respectively). **Note:** (→) PBS; (→) NC; (→) S-Fu; (→) TPGS-FA/NC; (→) TPGS-FA/NC; (→) 5-Fu; (→) PBS; (→) NC.

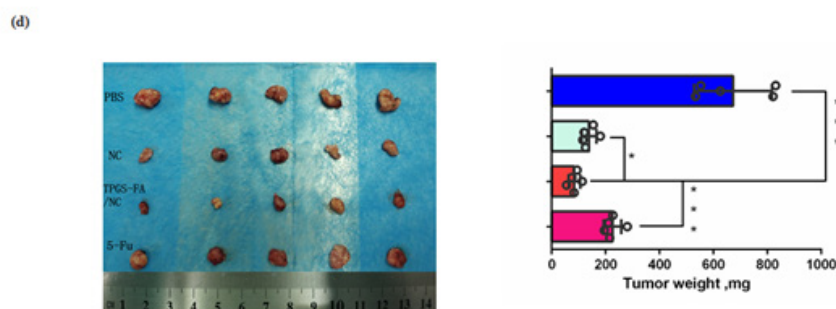


Figure 6d: Representative images of liver cancer tumours harvested from mice after treatments * $p<0.05$, ** $p<0.01$, *** $p<0.001$; $p=0.01, 8 \times 10^{-4}$ and 2×10^{-4} comparing.

Abbreviations: T: Tumour; Li: Liver; H: Heart; L: Lung; K: Kidney; S: Spleen; B: Brain

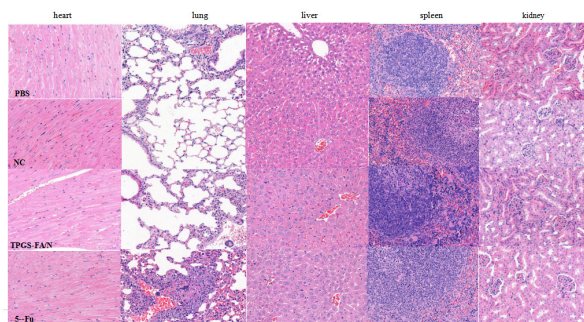


Figure7: HE stained in HCC mice bearing Huh7 xenograft specimens.

CONCLUSION

In this study, we revealed TPGS-FA/NC effects on Huh7 human HCC cell lines and their corresponding sphere cells *in vitro* as well as on a Huh7 cell xenograft model in BALB/c nude mice *in vivo*. Our results showed that TPGS-FA/NC significantly inhibited Huh7 cellular proliferation and colony formation. These data suggest a specificity of TPGS-FA/NC for hepatoma cells. We showed that TPGS-FA/NC suppressed the AQP3/CD133/STAT3 pathway in HCC cells, which was evidenced by reduced phosphorylation of STAT3, its upstream factor (AQP3) and two downstream signalling molecules, JAK1 and JAK2. Therefore, the downregulation of the AQP3/CD133/STAT3 pathway might have contributed to the inhibitory activity of TPGS-FA/NC on hepatic CSCs.

ETHICS APPROVAL AND CONSENT TO PARTICIPATE

Huh7 human hepatocellular carcinoma line did not require ethics approval for their use.

CONSENT FOR PUBLICATION

Not applicable.

AVAILABILITY OF DATA AND MATERIALS

All data generated or analysed during the present study are included in this article.

COMPETING INTERESTS

The authors declare that they have no competing interests.

FUNDING

This work was supported by the Guangxi Natural Science Foundation (2017GXNSFBA198021), Guangxi Key Laboratory of Zhuang and Yao Ethnic Medicine ((2014) No.32), Collaborative Innovation Centre of Zhuang and Yao Ethnic Medicine ((2013) No.20), and the Guangxi University for Nationalities Key Laboratory of National Medicine.

AUTHORS' CONTRIBUTIONS

Conceptualization, DL and HZ; Investigation, DL, JZ, and QZ; Methodology, DL, LS, and JZ; Supervision, HZ; Writing original draft, DL and SL; Reviewing and editing final version, DL and SL. All authors read and approved the final version of the manuscript.

ACKNOWLEDGMENTS

We are grateful to Professor Bernard at Guangxi University for revising the manuscript.

REFERENCES

1. Jemal A, Bray F, Center MM, et al. Global cancer statistics. *CA: Cancer J Clin*. 2011;61(2):69-90.
2. Zhou BB, Zhang H, Damelin M, et al. Tumour-initiating cells: Challenges and opportunities for anticancer drug discovery. *Nat Rev Drug Discov*. 2009;8(10):806-823.
3. Reya T, Morrison SJ, Clarke MF, et al. Stem cells, cancer, and cancer stem cells. *Nature*. 2001;414(6859):105-111.
4. Ma S, Chan KW, Hu L, et al. Identification and characterization of tumorigenic liver cancer stem/progenitor cells. *Gastro*. 2007;132(7):2542-2556.
5. Yamashita T, Honda M, Nakamoto Y, et al. Discrete nature of EpCAM⁺ and CD90⁺ cancer stem cells in human hepatocellular carcinoma. *Hepatology*. 2013;57(4):1484-97.
6. Yamashita T, Ji J, Budhu A, et al. EpCAM-positive hepatocellular carcinoma cells are tumour-initiating cells with stem/progenitor cell features. *Gastro*. 2009;136(3):1012-1024.
7. Xu X, Liu RF, Zhang X, et al. DLK1 as a potential target against cancer stem/progenitor cells of hepatocellular carcinoma. *Mol Cancer Ther*. 2012;11(3):629-638.
8. Chen Y, Yu D, Zhang H, et al. CD133⁺ EpCAM⁺ phenotype possesses more characteristics of tumour initiating cells in hepatocellular carcinoma Huh7 Cells. *Int J Biol Sci*. 2012;8(7):992.
9. Liu Y, Qi Y, Bai ZH, et al. A novel matrine derivate inhibits differentiated human hepatoma cells and hepatic cancer stem-like cells by suppressing PI3K/AKT signalling pathways. *Acta Pharmacol Sin*. 2017;38(1):120-132.
10. Wang X, Tao C, Yuan C, et al. AQP3 small interfering RNA and PLD2 small interfering RNA inhibit the proliferation and promote the apoptosis of squamous cell carcinoma. *Mol Med Rep*. 2017;16(2):1964-1972.
11. Huang X, Huang L, Shao M. Aquaporin 3 facilitates tumour growth in pancreatic cancer by modulating mTOR signalling. *Biochem Biophys Res Commun*. 2017;486(4):1097-1102.
12. Xiong G, Chen X, Zhang Q, et al. RNA interference influenced the proliferation and invasion of XWLC-05 lung cancer cells through inhibiting aquaporin 3. *Biophys Res Commun*. 2017;485(3):627-34.
13. Graziano AC, Avola R, Pannuzzo G, et al. Aquaporin1 and 3 modification as a result of chondrogenic differentiation of human mesenchymal stem cell. *J Cell Physiol*. 2018;233(3):2279-2291.
14. Zhou Y, Wang Y, Wen J, et al. Aquaporin 3 promotes the stem-like properties of gastric cancer cells *via* Wnt/GSK-3 β / β -catenin pathway. *Oncotarget*. 2016;7(13):16529.
15. Juuti-Uusitalo K, Delporte C, Grégoire F, et al. Aquaporin expression and function in human pluripotent stem cell-derived retinal pigmented epithelial cells. *Inves Opht Vis Sci*. 2013;54(5):3510-3519.
16. Wang Y, Wu G, Fu X, et al. Aquaporin 3 maintains the stemness of CD133⁺ hepatocellular carcinoma cells by activating STAT3. *Cell Death Dis*. 2019;10(6):1-5.
17. Wu W, Baxter JE, Wattam SL, et al. Alternative splicing controls nuclear translocation of the cell cycle-regulated Nek2 kinase. *J Biol Chem*. 2007;282(36):26431-26440.
18. Liu X, Gao Y, Lu Y, et al. Upregulation of NEK2 is associated with drug resistance in ovarian cancer. *Oncol Rep*. 2014;31(2):745-754.
19. Li D, Liu S, Zhu J, et al. Folic acid modified TPGS as a novel nano-micelle for delivery of nitidine chloride to improve apoptosis induction in Huh7 human hepatocellular carcinoma. *BMC Pharmacol Toxicol*. 2021;22(1):1-1.